



## Original Research Paper

# Slow pyrolysis of cork granules under nitrogen atmosphere: by-products characterization and their potential valorization

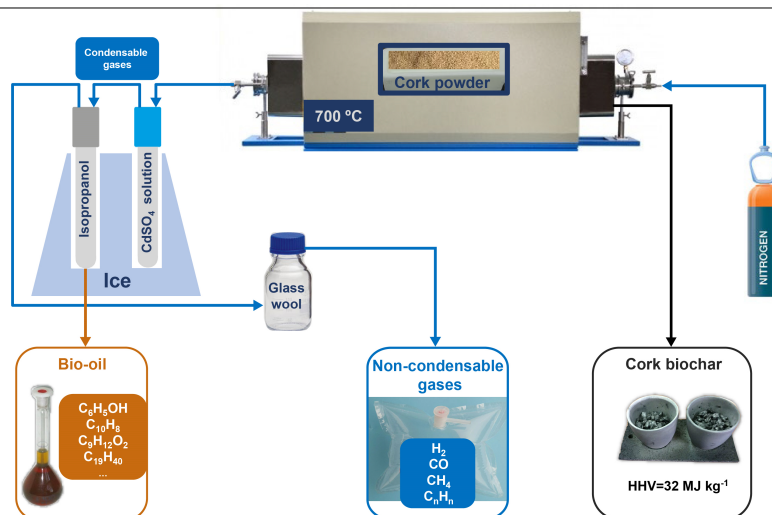
Paula A. Costa, M. Alexandra Barreiros, Ana I. Mouquinho<sup>‡</sup>, Pedro Oliveira e Silva, Filipe Paradela, Fernando A. Costa Oliveira\*

LNEG - Laboratório Nacional de Energia e Geologia I.P., LEN - Laboratório de Energia, Estrada do Paço do Lumiar 22, 1649-038 Lisboa, Portugal.

## HIGHLIGHTS

- *Quercus Suber* L. pyrolysis by-products including biochar and bio-oil were investigated.
- Cork biochar belonged to class 1 (C>60%) with HHV of 32 MJ kg<sup>-1</sup>.
- Cork bio-oil consisted of long-chain hydrocarbons (from C11 to C24).
- H<sub>2</sub> yield increased from 0 to 58% by increasing temperature from 400 and 700°C, respectively.
- Total hydrocarbon gases dropped from 74 to 24% by raising T from 500 to 700°C.

## GRAPHICAL ABSTRACT



## ARTICLE INFO

### Article history:

Received 15 December 2021  
Received in revised form 16 February 2022  
Accepted 18 February 2022  
Available online 1 March 2022

### Keywords:

Pyrolysis  
Cork (*Quercus suber* L.)  
Bio-oil  
Biochar  
Bioenergy  
Sustainability

## ABSTRACT

Cork granules (*Quercus suber* L.) were slowly pyrolyzed at temperatures between 400-700 °C and under N<sub>2</sub> flow. While preserving its structure, some cells of the cork biochar became interconnected, allowing such carbon residue to be used as templates for manufacturing ceria redox materials. The pyrolytic char morphology was similar to that of the natural precursor. The produced cork biochar belonged to Class 1 (C > 60%) and possessed a high heating value of 32 MJ kg<sup>-1</sup>. Other pyrolysis-derived compounds were identified and quantified through GC-FID and GC-MS analyses. The yield of gases released during cork pyrolysis was strongly dependent on the temperature used due to the thermal decomposition reactions involved in the degradation of cork. In particular, rising pyrolysis temperature from 500 to 700 °C resulted in reducing the total hydrocarbon gases from 74 to 24 vol%. On the other hand, the yield of H<sub>2</sub> increased from 0 to 58% by increasing the pyrolysis temperature from 400 to 700 °C. Due to the presence of suberin in cork, the composition and yield of bio-oil could be regulated by the pyrolysis temperature. Cork bio-oil was found to consist of long-chain hydrocarbons (from C11 to C24). The bio-oil resulting from the slow pyrolysis of cork residues is suitable as an appropriate feedstock for producing aliphatic-rich pyrolytic biofuels or as a source of olefins. Overall, the findings of this study suggest that *Quercus suber* L. could be a promising feedstock for biochar and biofuel production through the pyrolytic route and could contribute to the environmental and economic sustainability of the cork production industry.

© 2022 BRTeam. All rights reserved.

\* Corresponding author at: Tel.: +351 21 092 4600

E-mail address: [fernando.oliveira@lneg.pt](mailto:fernando.oliveira@lneg.pt)

<sup>‡</sup> Present Address: Advanced Functional Materials for Micro and Nanotechnologies Team, CENIMAT – i3N - Institute for Nanostructures, Nanomodelling and Nanofabrication, Department of Materials Science, Faculty of Sciences and Technology, Nova School of Science and Technology, Campus da Caparica, 2829-516 Caparica, Portugal.

## Contents

1. Introduction.....	1563
2. Materials and Methods.....	1565
2.1. Cork samples.....	1565
2.2. Thermogravimetric analysis.....	1565
2.3. Pyrolysis process.....	1565
2.4. Chromatographic analysis.....	1565
2.5. Characterization of biochar products.....	1565
2.6. Cork morphology.....	1565
3. Results and Discussion.....	1565
3.1. Structural characterization of cork.....	1565
3.2. Thermogravimetric data.....	1566
3.3. Pyrolysis data.....	1567
3.3.1. Non-condensable gas composition.....	1567
3.3.2. Condensable gas fraction composition.....	1567
3.3.3. Solid fraction characterization.....	1568
4. Conclusions and Prospects.....	1569
Acknowledgements.....	1569
References.....	1570

## Nomenclature and abbreviations

APCOR	Associação Portuguesa da Cortiça (Portuguese Cork Association)
DSC	Differential Scanning Calorimetry
DTG	Differential Thermogravimetry
EPA	U.S. Environmental Protection Agency
EtOH	Ethyl alcohol
FAO	Food and Agriculture Organization
FEG	Field Emission Gun
FID	Flame-Ionization Detection
GC-FID	Gas Chromatography with Flame Ionization Detector
GC-MS	Gas Chromatography-Mass Spectrometry
HHV	Higher Heating Value ( $\text{MJ kg}^{-1}$ )
IBI	International Biochar Initiative
ITC	International Trade Centre
Py-GC/MS	Pyrolysis-Gas Chromatography/Mass Spectrometry
SEM	Scanning Electron Microscopy
TGA	Thermogravimetric Analysis
3DOM	Three-Dimensionally Ordered Macroporous Structure
VOC	Volatile Organic Compound

## 1. Introduction

Cork is the bark protective biological tissue of oak trees. The cork oak (*Quercus suber* L.) forests in several Mediterranean countries are estimated to cover an area of around 2 million ha. In Portugal, oak trees occupy an area of circa 720 thousand ha (according to the data available in 2015), corresponding roughly to 20% of the country's forest area (APCOR, 2020). World cork production is about 200 thousand tons. Portugal is the market leader in production, with 46% and 85 thousand tons and about 40 million cork stoppers/d. According to the International Trade Centre (ITC), Portugal was the world leader in terms of cork exports (62.4% share) in 2017 (APCOR, 2019), with the total world cork exports reaching 1,568.7 million euros (Fig. 1). Although cork is mostly used for sealing wine bottles (around 40 vol%) to preserve the wine for long-term storage, other cork-based products (35 wt%) include agglomerates, flooring and insulation panels (Silva et al., 2005), coverings, cubes, plates, sheets and strips, insulation and surfacing boards as well as polymer matrix composites (Gil, 2009; Fernandes et al., 2011; Martins and Gil, 2020).

The residues resulting from cork processing (25 wt%) is, 1) cork powder having particle dimensions lower than 0.25 mm, which is being mainly used as a combustion fuel and for linoleum production (Gil, 1997), and 2) black

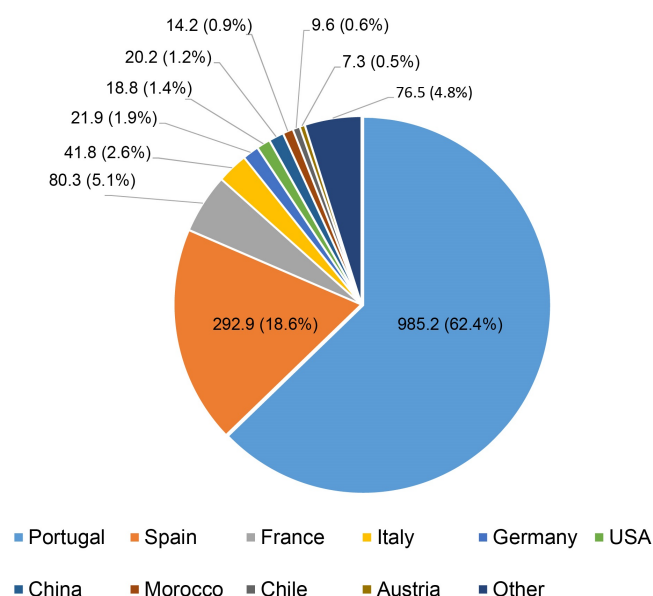


Fig. 1. World cork exports by country (Million €) and country shares (%) in 2017.

condensate (consisting of volatile compounds released during the production of black agglomerates). These cork powder and black condensate residues account for ca. 40000 and 2500 tons/yr in Portugal (Gil, 1997), respectively, and are currently being burnt to produce heat (Sousa et al., 2006). Bearing in mind the amounts of residues generated and their composition, one should rethink and upgrade their potential use as a renewable source of value-added chemicals. To this end, the novel applications for cork by-products require detailed knowledge of their composition and structure, which lags far from being completely attained. Several depolymerization methods, namely alkaline hydrolysis, methanolysis, alcoholysis, reduction cleavage, and ionic liquids extraction, are employed to recover suberin (the major cork constituent, accounting for ca. 40 wt%) to valorize cork wastes and increase its extraction yields (Ferreira et al., 2012). Cork by-products are also an important source of multiple bioactive components, such as phenolic acids, terpenoids, and tannins for different pharmaceutical and cosmetic applications (Carriço et al., 2018). Cork biomass also has commercial value as a source of energy and biofuels (Nunes et al., 2013; Mateus et al., 2016).

Lignocellulosic biomass is generally a sustainable, environmentally benign, cost-effective alternative to fossil fuels and could serve as a carbon-neutral renewable resource for biofuels and chemicals production. This has led to the development of thermochemical processes suitable to transform biomass into usable products, namely combustion, gasification, pyrolysis,

and liquefaction (Haq et al., 2021). In pyrolysis, the biomass is thermally decomposed to low molecular mass products, either into liquid (bio-oil), solid (biochar), or fuel gas (e.g.,  $H_2$ ), depending on process conditions. Several review articles have been devoted to biomass pyrolysis (Kan et al., 2016; Wang et al., 2020; Xia et al., 2021).

Teixeira et al. (2017) investigated the effect of cork granules size on the char yield produced after slow pyrolysis. Carbonization would be a more appropriate term when the major by-product is a carbon char, while the term pyrolysis is more often used to describe processes in which a bio-oil is produced. Higher heating rates and shorter residence times maximize liquid yields, whereas lower heating rates increase the production of residual char. Marques and Pereira (2014) demonstrated that flash pyrolysis using Py-CG-MS (FID) was a suitable analytical tool for analyzing aliphatic bio-oils produced from cork. However, they argued that the production of aliphatic rich bio-oils from cork required temperatures in the range 800–900 °C, jeopardizing its economic feasibility. Other studies pointed out the benefits of gasification for the drainage and efficient reprocessing of cork industry wastes (Al-Kassir et al., 2010). Hence, converting cork into a pyrolytic liquid, typically called bio-oil, is a promising route with yields, composition, and properties directly related to feedstock and pyrolysis conditions (Mohan et al., 2006). However, the current knowledge on cork fast pyrolysis is still scarce. Nonetheless, data on bio-oil production from cork using fast pyrolysis highlight that cork and wood pyrolysis bio-oil compositions are similar; the bio-oil yield from cork is much lower though, i.e., about half of that resulting from wood at 550 °C (Marques and Pereira, 2014). This is ascribed to the fact that cork from *Q. suber* L. is anatomically and chemically different from wood. It possesses a regular structure based on small closed cells, with a cell wall structural average composition consisting of suberin 43±6%, lignin 22±3%, polysaccharides 19±3%, and extractives 16±4% (Pereira, 2013).

Attention is drawn to the need of improving bio-oil quality by minimizing its undesirable properties, namely high water content, high viscosity, high corrosivity (pH ranging from 3.5 to 4.2), and chemical instability, thereby producing renewable fuels suitable for direct use in conventional engines (Pinto et al., 2018; Iliopoulou et al., 2019). Therefore, upgrading bio-oil is essential before it can be used commercially. These issues have led to an increasing interest in utilizing slow pyrolysis to valorize biomass, producing mainly char, which has several applications (Zhang et al., 2019). In this context, it is important to also investigate bio-oil production from cork wastes through slow pyrolysis, despite being produced in a much lower quantity. Regardless of the route used, being able to recover and valorize this by-product to maximize the material and energy balance of the overall process will minimize the environmental footprint and ensure economic sustainability since millions of tons per year of bark residues are generated by forest-based activities and industries (FAO, 2020).

As mentioned earlier, during pyrolysis, the organic macromolecules are thermally decomposed in sequential reactions giving rise to main four different fractions: the aqueous fraction (condensable water vapor), the organic fraction (condensable organic vapors, giving rise to a liquid bio-oil), the solid fraction (carbonaceous residue mostly constituted of black carbon) and the gas fraction (low molecular weight products, which have a moderate vapor pressure at room temperature). The quantity of these four main products depends on the chemical composition of the biomass and the operating conditions of the process. The pyrolytic decomposition of cork is illustrated in Figure 2.

Thermochemical liquefaction of renewable bio-resources, such as cork dust, for the production of biofuels, has also attracted much attention in recent years (Mateus et al., 2016). In this context, the use of biomass-derived chemicals in the synthesis of polymers traditionally made from petroleum-based resources, namely polyurethane, is being envisaged (Yona et al., 2014). The production of activated carbons from cork powder wastes was also investigated (Cardoso et al., 2008). Although the results of these investigations are promising on a small scale, further work is required to reduce costs compared with fossil-based sources to penetrate the energy markets.

In the present work, the characteristics of the biofuel byproduct resulting from the slow pyrolysis process of a low-cost residue of the cork industry (cork granules of *Q. suber* L.) were investigated. It should be highlighted that the few studies conducted on slow pyrolysis of cork were mainly concerned with the characterization of char and syngas since they are the main products (Teixeira et al., 2017), and the data on the resulting bio-oil was only found for fast pyrolysis of cork (Marques and Pereira, 2014). Hence, the goal of this work was twofold: firstly, to obtain a biochar while maintaining the regular three-

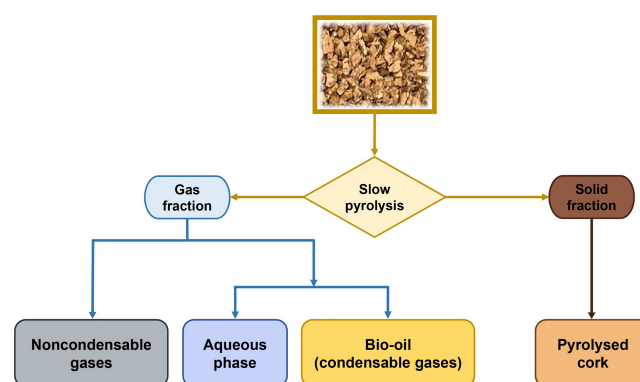


Fig. 2. Schematic presentation of the slow pyrolysis process of the cork.

-dimensional structure of cork, which could be used for producing ceria catalysts with high surface area for green hydrogen generation via the thermochemical cycle, using concentrated solar energy as the heating source (Oliveira et al., 2020).

Secondly, to characterize the pyrolysis by-products in the temperature range of 400–700 °C as a feedstock for the production of activated carbon, biofuels, and olefins. This was accomplished by chemical analysis of the pyrolysis process through gas chromatography (GC) coupled with both flame-ionization detection (FID) and mass spectrometry (MS) for precise identification of non-condensable gas species and the bio-oil resulting from the pyrolysis of cork. To the best of our knowledge, this is a pioneering work on the chemical characterization of bio-oil resulting from the slow pyrolysis of cork residues as a potential feedstock for producing aliphatic-rich pyrolytic biofuels or as a source of olefins. Such data on the bio-oil characteristics resulting from slow pyrolysis of cork wastes were evaluated for the first time, as highlighted in Table 1.

Table 1.

Comparison of the present work with the previously published works on pyrolysis of biomass wastes.

Technology		Characterization method		By-product analysis		Ref.
Fast pyrolysis	Slow pyrolysis	Py-GC-MS	GC-MS	Char yield & HHV	Bio-oil composition	
×	√	×	×	√	×	Teixeira et al. (2017)
√	×	√	×	×	√	Marques and Pereira (2014)
×	×	×	√	√	×	Al-Kassir et al. (2010)
×	×	×	×	√	×	Mateus et al. (2016)
√	×	×	√	√	×	Mohan et al. (2006)
×	×	×	√	×	√	Pinto et al. (2018)
×	×	√	√	√	√	Iliopoulou et al. (2019)
×	×	×	×	√	√	Zhang et al. (2019)
×	√	×	√	√	√	This work

√ Included × Not included

## 2. Materials and Methods

### 2.1. Cork samples

The raw material under investigation was cork granules produced by Amorim Cork Composites S.A. (Portugal), resulting from the processing, trimming, and shaping of cork stoppers for wine. Granulated cork had a particle size greater than 2 mm and a density of 120 kg m<sup>-3</sup>. It was dried in an oven set to 100 °C until no change in mass was observed.

### 2.2. Thermogravimetric analysis

Thermogravimetric (TGA) analysis was used to investigate the pyrolysis of cork by measuring the mass changes as a function of temperature on a thermobalance (TG/DTA/DSC SetSys Evolution 1750, Setaram, France), at atmospheric pressure, under an argon flow of 100 NmL min<sup>-1</sup>, from room temperature up to 600 °C with heating and cooling rates of 5 °C min<sup>-1</sup>. Owing to its low density, only 20 mg of cork sample could be tested in the TG balance filling up the available alumina crucibles placed inside the furnace chamber. Therefore, it was not possible to perform mass spectrometry analysis of the resulting gas products.

### 2.3. Pyrolysis process

The pyrolysis of cork granules took place in a horizontal electric furnace (Termolab – Fornos Eléctricos, Lda.), using Kanthal Super molybdenum disilicide (MoSi<sub>2</sub>) heating elements, capable of reaching temperatures as high as 1700 °C. The reaction took place inside an alumina tube with 1 m long, 80 mm outer diameter, and 70 mm inner diameter (Degussit AL 23, 99.5% purity). Sealed water-cooled clamping flanges were used at both ends to allow either vacuum or controlled atmosphere to be employed. Temperature control was made by a Type-B thermocouple (70%Pt/30%Rh–94%Pt/6%Rh, by weight), located in the vicinity of the reaction tube, connected to an automatic temperature controller (Eurotherm 818). Each pyrolysis was made using approximately 2 g of fine granule natural cork, heated at a rate of 5 °C min<sup>-1</sup> up to 700 °C for 30 min, and then cooled to room temperature at 5 °C min<sup>-1</sup>. The pyrolysis process was conducted in a continuous nitrogen flow (10 NL min<sup>-1</sup>) to prevent the combustion of cork. During pyrolysis, the gases released in the process were collected at given temperatures for suitable bags (Tedlar SKC Inc.) at the outlet of the reaction tube. Since these collections were made during the pyrolysis process rather than at the end, a special procedure had to be implemented to collect only gaseous compounds at room temperature (non-condensable gases). Both cleaning and collection systems were intended to condense unwanted gases and prevent them from entering the sample collection bag (Fig. 3).



**Fig. 3.** Schematic representation of the experimental setup used to perform the pyrolysis of cork and collection system for handling condensable and non-condensable gas fractions.

The gas fraction produced during pyrolysis (condensable and non-condensable gases) passed first through a 150-mL cadmium sulfate solution impinge bottle containing 0.16 M CdSO<sub>4</sub> and 0.0015 M H<sub>2</sub>SO<sub>4</sub>, following the test method used for the determination of hydrogen sulfide content of fuel gas streams in petroleum refineries (EPA, 2017), to condense any traces of sulfur produced, followed by a 150-mL isopropanol impinge bottle to condense the heaviest hydrocarbons. Then a glass wool flask was used to retain solid particles, and finally, the gaseous flow (non-condensable gases) was stored in

the collection bags. To enhance gas condensation, the impingers were placed in an ice-bath box to keep the cleaning solutions at a low temperature (between 4 and 10 °C). Each gas sample was taken at 400, 500, 600, and 700 °C for 15 min.

### 2.4. Chromatographic analysis

The gases released in the pyrolysis process were analyzed by GC to determine the content of hydrogen, nitrogen, carbon dioxide, carbon monoxide, alkenes, and alkanes (methane, ethylene, ethane, propane, butane, and cis-2-butene). The collected gases were manually injected into an Agilent/HP 6890 gas chromatograph equipped with a gas sampling valve, two filling columns (Molecular Sieve 5A and Porapak Q), and two detectors (Thermal Conductivity Detector and Flame Ionization Detector) mounted in series.

Each gas sample was heated at 40 °C for 17 min followed by heating at 15 °C min<sup>-1</sup> to 185 °C for 43 min. The carrier gas used was argon at a constant flow of 18.5 mL min<sup>-1</sup>.

Quantitative analysis of the gaseous compounds was determined by comparing the peak area of each compound in the sample with the area of that compound in calibration mixtures, according to an in-house developed method. These concentrations were determined on a nitrogen-free basis, assuming that this component came mainly from the atmosphere (carrier gas), and the contribution of cork was negligible.

On the other hand, the liquid phase (condensed gases in isopropanol impinge bottle) produced by the pyrolysis of cork was also analyzed by a gas chromatograph equipped with a mass spectrometer (LECO Instruments PEGASUS III). The liquid product fraction was distilled at 40 °C under a low vacuum (10<sup>-3</sup> mbar) to remove the solvent. The liquid pyrolysis products analyzed thus correspond to the residue remaining in the distillation flask. This residue was further diluted in 1 mL of isopropanol and analyzed by GC-MS.

The GC-MS was equipped with a DB-5 column. Each sample was heated at 40 °C for 10 min followed by heating at 5 °C min<sup>-1</sup> to 200 °C. The carrier gas used was helium at a constant flow of 1.5 mL min<sup>-1</sup>. The injection mode was splitless, and the transfer line temperature was 250 °C. The identification of the compounds was performed using the National Institute of Standards and Technology (NIST) 's mass spectral search program. The gas fraction composition was determined by direct injection of the samples, which did not involve any sample treatment. The analysis was repeated three times, and the value presented is the mean of the obtained values. The standard deviation was lower than 5%. The correlation coefficient of the calibration curves was at least 0.999. Four standard calibration gas mixtures (supplied with a Certificate of Analysis) were used, with different concentrations of each compound.

### 2.5. Characterization of biochar products

The elemental (CHN) analysis was performed in duplicate using an Elemental Vario Macro Cube analyzer. The sulfur and chlorine contents were determined using a Parr calorimetric pump and a Dionex ICS 3000 ion chromatography system. The char's higher heating value (HHV) was measured in duplicate by bomb calorimetry (Parr model 6400 calorimeter).

### 2.6. Cork morphology

To check for morphology changes, samples were observed by scanning electron microscopy (SEM) using a Philips XL30 FEG (field emission gun) before and after pyrolysis. SEM secondary electron images were obtained at an acceleration voltage of 5-10 kV.

## 3. Results and Discussion

### 3.1. Structural characterization of cork

In general, the cork is formed by individual cells, which are hexagonal prisms without intercellular spaces, placed in successive layers forming a honeycomb-like structure (Lagorce-Tachon et al., 2018; Le Barbenchon et al., 2018). However, when observed three-dimensionally considering the three directions of the tree growth (radial, axial and tangential), cork cells



arrange in a different appearance (Fig. 4). In the axial and tangential sections, the cells appear rectangular, and in the radial direction, the cork cells appear as hexagons with a honeycomb structure.

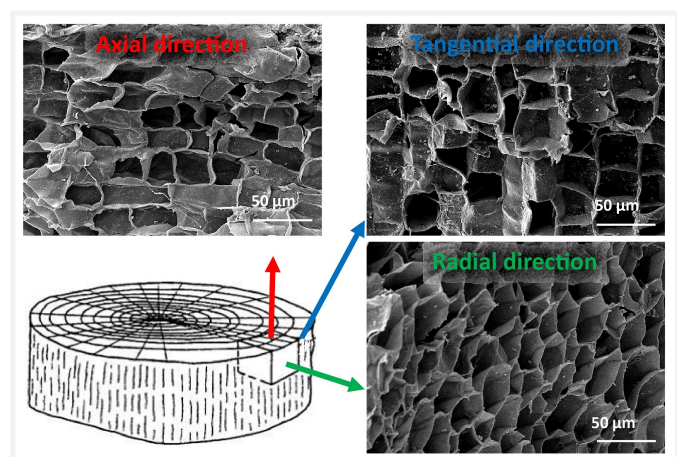


Fig. 4. Morphology of the cork cells in the corresponding growth directions relative to the cork tree trunk.

Typical SEM micrographs of the natural and pyrolyzed material with the characteristic alveolar structure of this material are shown in Figure 5. The microstructure of natural cork has hollow closed cells whose walls are visible in Figures 5a, b, and c. Upon pyrolysis, the porous morphology of the carbon material is preserved. However, some large pores/cracks were formed within cell walls, and certain cell walls were removed, which increased the material's porosity, creating an interconnect cell network and making infiltration possible. These attributes consequently improve the suitability of the cork materials to serve as a scaffold for the production of ecoceramics (Oliveira et al., 2020). Figures 5d, e, and f corroborate this finding, even though the micrographs of the pyrolyzed cork were taken from the tangential direction sections, whereas the SEM images of the natural cork were from the axial direction sections.

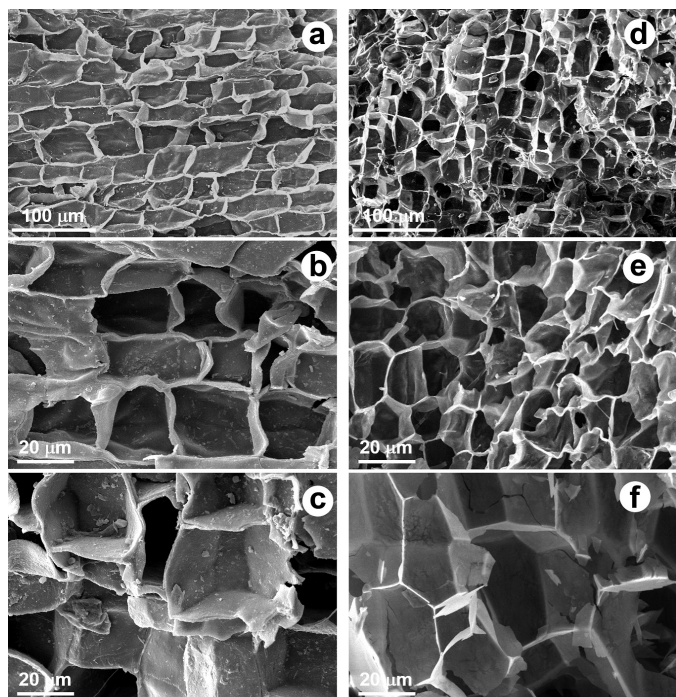


Fig. 5. SEM micrographs of (a, b, c) the natural and (d, e, f) the pyrolyzed cork.

### 3.2. Thermogravimetric data

The TG thermogram obtained upon heating the cork sample in the argon atmosphere is shown in Figure 6, where two distinct events could be observed during the thermal degradation. The first occurred in the temperature range of 280-350 °C, which could be attributed to the degradation of both hemicelluloses and cellulose (Yao et al., 2008). The second event took place at  $T > 350$  °C, corresponding to the more pronounced degradation of both suberin and lignin owing to their three-dimensional and heavily cross-linked structures (Yang et al. 2004). In the pyrolysis of lignocellulosic materials, lignin is the main element responsible for the char produced (Órfão et al., 1999). The mass loss recorded in the temperature range of 285 °C and 500 °C was ca. 10 mg, corresponding to the total mass loss. In other words, 47% of the total mass was converted into char (total sample mass of 19 mg), indicating the acceptable potential of cork to produce char. More specifically, the highest mass loss rates were recorded at around 315 and 445 °C, respectively. Above 280 °C, devolatilization reactions involving degradation of extractives, namely triterpenes like betulinic acid, cerine, and friedelin (Sousa et al., 2006), long-chain alkanes and alkanols (Castola et al., 2005), polysaccharides (e.g., hemicelluloses), and lignin (up to a certain extent) took place. The degradation of suberin, cellulose and the remaining lignin occurred at  $T > 350$  °C. At lower temperatures, lignin degradation is attributed to the cleavage of alkyl-aryl ether linkages, whereas the cleavage of aromatic rings and C-C bonds causes degradation at higher temperatures (Wen et al., 2013).

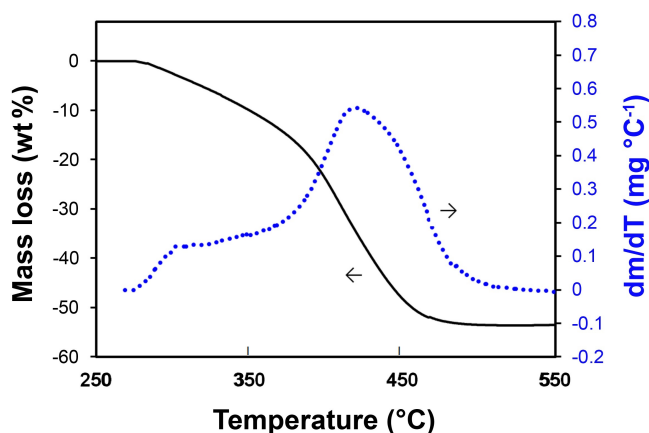


Fig. 6. Typical TG thermogram obtained for cork *Quercus suber* L. raw powder.

Details about the cork chemical composition are reviewed elsewhere (Pereira, 2015; Leite and Pereira, 2017; Costa et al., 2019). The mechanisms of cork degradation have been extensively studied using TGA and differential scanning calorimetry (DSC) techniques (Şen et al., 2014). The chemical changes may be summarized as follows: extractives (namely dichloromethane and EtOH) are volatilized first, then hemicelluloses are degraded, while lignin (mainly Klason type) and suberin are the most durable components and last to be degraded either under flowing oxygen, nitrogen or air atmospheres, as corroborated by FTIR spectroscopy analysis (Şen et al. 2012). Although an argon atmosphere was used in the present work, the results acquired were in good agreement with those reported by Fernandes et al. (2015) for cork granules heated from 50 to 600 °C, at a heating rate of 10 °C min<sup>-1</sup>, under nitrogen atmosphere. In a work by Rosa and Fortes (1988), cork granules showed an initial degradation temperature ( $T_{onset} = 246$  °C) slightly lower than that observed in Figure 6. Temperature-induced effects were also observed in the cellular structure of cork by Pereira (1992) upon heating in air. At the early stages of the heating treatment, cell expansion and flattening of wall corrugations occurred. Around 250 °C, the cell walls were found to stretch, and consequently, their thickness was reduced, attaining a maximum cell volume increase corresponding roughly to a factor of 2, as observed by SEM analysis

(Pereira, 1992). Although no explanation was provided by the authors, thermal expansion of the cells is responsible for the increase in cell volume. Considering that the cells are closed, the entrapped air dilates, thereby causing plastic deformation of the cell walls. Otherwise, upon cooling, the deformed cells would recover their original size. This observation corroborates the finding that the pyrolyzed cork contains collapsed cell walls (Fig. 5d), thereby allowing the formation of an interconnected cells network, which can thus be infiltrated with a ceramic slurry. While the rectangular side walls were maintained to hold together the three-dimensionally ordered macroporous (3DOM) cellular cork structure, the rear hexagonal walls were pierced repeatedly through the structure, unlike in the original cork structure, thus allowing the resulting carbon skeleton to be infiltrated with an aqueous  $\text{CeO}_2$  precursor, and then heated at 1600 °C for 3 h to produce the ceria ecoceramic suitable for green  $\text{H}_2$  production via the concentrated solar thermochemical cycle (Oliveira et al., 2020).

### 3.3. Pyrolysis data

As defined earlier, pyrolysis is a thermochemical decomposition of a given raw material into gaseous, liquid, and solid products produced in the absence of an oxidizing atmosphere. In this process, large complex biomass molecules are broken down into smaller and simpler molecules. The main goal of pyrolysis has been the production of a liquid (bio-oil) to be used as fuel. However, nowadays, the interest in biochar production by biomass pyrolysis is also substantial. To produce biochar, slow pyrolysis, in which biochar production is the primary goal, needs to be performed. This process occurs over an extended period, allowing the condensable vapor to be converted into char and non-condensable gases (Bento et al., 1992; Lu et al., 2008). However, a small amount of bio-oil (the condensable gas fraction) is also produced (Dhyani and Bhaskar, 2018). These products were characterized, and the results are discussed in the following sections.

The pyrolysis process of cork can be understood based on the thermal decomposition of its three main biomass components: suberin, lignin, and polysaccharides (hemicelluloses), which react differently upon heating (Ronsse et al., 2015; Silva et al., 2005). Suberin is the main chemical component of cork from *Q. suber* L., accounting for about 40% of its mass. Cellulose represents only around 9% of cork cell walls, whereas it could amount to 40-50% in other woods and barks (Pereira, 1988). On the other hand, lignin content in cork is 22%, on average, which is similar to the values observed for other wood or bark materials from broadleaved trees.

#### 3.3.1. Non-condensable gas composition

The characterization of the non-condensable gas fractions was carried out by GC to evaluate the effect of temperature on the composition of gases resulting from the pyrolysis of cork. The gas compositions from the pyrolysis of cork at 400, 500, 600, and 700 °C are given in Figure 7.

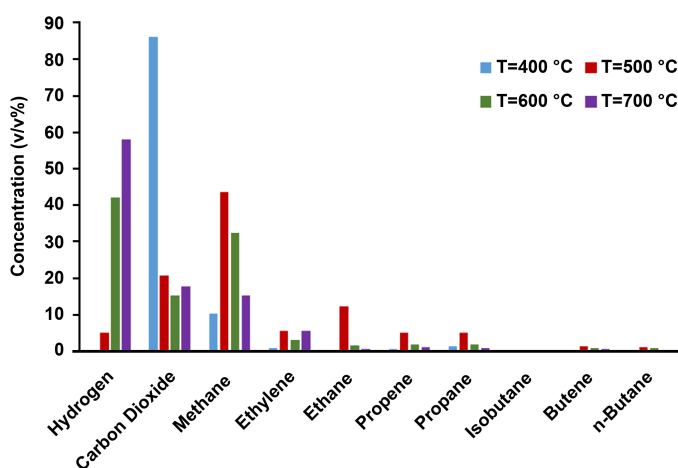


Fig. 7. Composition of the non-condensable gas fraction resulting from the pyrolysis process of cork at given temperatures.

The data represent the volume percentages of each compound present in the gas product on a nitrogen-free basis. The main components detected were hydrogen, carbon dioxide, and methane. The gaseous compounds are generated thermally in the pyrolysis process, so hydrogen and methane are formed from volatile matter cracking and depolymerization reactions, and CO and  $\text{CO}_2$  from decarboxylation and depolymerization reactions. Other hydrocarbons ( $\text{C}_2$  to  $\text{C}_4$ ) were detected in small amounts. Unexpectedly, the presence of CO was not detected. During the biomass pyrolysis, oxygen may be removed from the biomass through different chemical reactions: decarboxylation, decarboxylation, and hydrodeoxygenation to produce  $\text{CO}_2$ , CO,  $\text{H}_2$ ,  $\text{H}_2\text{O}$ . This implies that the experimental conditions used and the type of reactor did not favor the decarboxylation reaction. This reaction is more unlikely to occur in non-catalytic processes (Fukuyama et al., 2014).

In studies using other types of biomasses (e.g., pomegranate seeds, straw, olive waste, birch, and bagasse), CO was detected in high concentrations, typically in the range from 20 to 40% (Encinar et al., 2000; Uçar and Karagöz, 2009).

Reaction temperature has a significant influence on pyrolysis gas product yield and composition. With increasing pyrolysis temperature, thermal degradation and devolatilization of biomass are favored. Concurrently, a series of secondary reactions (such as decarboxylation, decarbonylation, dehydrogenation, deoxygenation, and cracking) involving the produced volatiles takes place to form the pyrolysis gas product (Uçar and Karagöz, 2009). Some studies were performed on the effect of reaction temperature on the pyrolysis gas product (Encinar et al., 2000; Hu and Gholizadeh, 2019), and overall, the major positive impact of higher temperatures on the yield of gases generated is especially observed in the case of hydrogen. In fact, in the present study, it was noticed that the amount and composition of non-condensable gases through the pyrolysis of cork was temperature-dependent, and three main peaks of  $\text{H}_2$ ,  $\text{CO}_2$ , and  $\text{CH}_4$  were identified.

The hydrogen yield increased from 0 to 58% by increasing temperatures from 400 to 700 °C, respectively. Hydrogen emission is related to the bond breaking of functional groups in the hemicellulose branches at around 450 °C. At higher temperatures, the breakdown of lignin's monomeric units occurs and, above 600 °C, hydrogen generation is due to the cracking of the tar. This finding is corroborated by observations made by Encinar et al. (2000) when studying the effect of temperature on the gas composition resulting from the pyrolysis of the crop *Cynara cardunculus* L. at temperatures within the range 300-800°C. Other studies showed a similar tendency (Wang et al., 2007; Hu and Gholizadeh, 2019).

On the other hand, the  $\text{CO}_2$  content was much higher at low temperatures. At 400°C, the gaseous products consisted mainly of  $\text{CO}_2$ . The release of  $\text{CO}_2$  decreases with increasing temperature up to 500°C: the highest peak of 86% is recorded at 400 °C, due to the degradation of both cellulose and hemicelluloses. At higher temperatures,  $\text{CO}_2$  emission is related to cracking and reforming of COOH, C=O, and OH bonds located in the aliphatic phenylpropane chains of lignin. These results suggest that pyrolysis at lower temperatures preserves hydrogen atoms in biomass while removal of oxygen atoms occurs in the form of  $\text{CO}_2$ . These results were similar to those reported for the pyrolysis of pomegranate seeds at 400, 500, 600, and 800°C in a fixed bed reactor (Uçar and Karagöz, 2009). Attention is drawn to the fact that the  $\text{CO}_2$  content obtained at higher temperatures was much higher than in the present study, owing to the use of a different biomass and type of reactor (Encinar et al., 2000).

The emission of methane is related to the thermal degradation of lignin. At 400 °C, the methoxyl ( $\text{O-CH}_3$ ) and methyl ( $\text{CH}_3$ ) groups break down, and at higher temperatures, the breakage of the aromatic rings does occur. Rising temperature from 500 up to 700 °C resulted in the reduced content of the total hydrocarbon gases ( $\text{CH}_4$ ,  $\text{C}_2\text{H}_6$ ,  $\text{C}_2\text{H}_4$ ,  $\text{C}_2\text{H}_2$ ) in the pyrolysis gas from 74 to 24 vol.%. This observation is in good agreement with data reported by Zanzi (2001), who performed the pyrolysis of straw, straw pellets, olive waste, birch, and bagasse at various temperatures.

#### 3.3.2. Condensable gas fraction composition

In this work, the liquid phase (condensed gases in isopropanol impinge bottle) produced by the pyrolysis of cork was analyzed by GC-MS. Mass spectrometry has proved to be a convenient technique for the analysis of

the thermal degradation of cork in a vacuum furnace (Bento et al., 1992). No such data could be found in an inert atmosphere.

The biomass nature has a relevant and distinct effect on the final pyrolysis product related to lignocellulosic composition. Cork is anatomically and chemically different from wood. The wood-derived bio-oils have complex compositions with more than 300 compounds, including water, pyrolytic lignin, and a wide range of oxygenated organic compounds with many functional groups (e.g., acids, aldehydes, alcohols, alkenes, ethers, ketones, and phenols), which are derived from polysaccharides and lignin thermal degradation.

The hydrocarbon fraction of cork bio-oil was found to consist of long-chain hydrocarbons (from C11 to C24), as shown in Figure 8, together with the linear alkane and 1-alkene, as indicated by the two peaks observed at each carbon number. The main hydrocarbons detected were C12 to C22. The presence of such long-chain hydrocarbons (alkanes and alkenes) in the liquid fraction is in good agreement with the products of the pyrolysis process in a continuous flow of N<sub>2</sub> (Fig. 9).

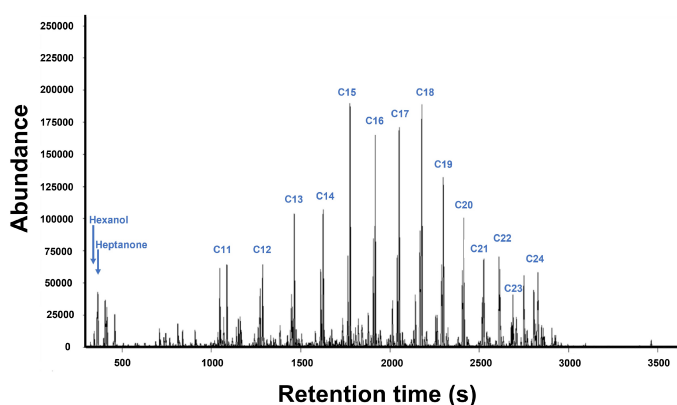


Fig. 8. GC-MS chromatogram of hydrocarbon compounds in the liquid fraction obtained by pyrolysis of cork.

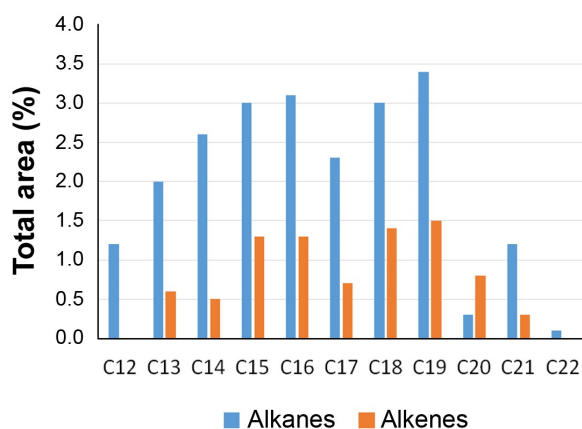


Fig. 9. Liquid fraction long-chain functional groups in cork bio-oil.

In the flow mode operation, the cracking is not favored owing to the continuous release of the products formed so that long-chain hydrocarbons are produced instead of short-chain compounds. Moreover, the structure of suberin in cork consists of a polyester structure composed of long-chain fatty acids, hydroxyl fatty, and phenolic acids, linked by ester groups. This is consistent with the macromolecules identified in this fraction. It is also necessary to note that bio-oils contain many non-volatiles which are not GC-eluted (Basu, 2018). Besides, small proportions of oxygenated compounds such as alcohols (hexanol) and ketones (heptanone) generated from cellulose pyrolysis were also detected in the liquid fraction. These results are in good agreement with

those reported for other bio-oil products (Chen, 2015; Guedes et al., 2018; Pinto et al., 2018).

The chemical composition of the bio-oil produced during slow pyrolysis could hardly be found, as most data refer only to fast pyrolysis. Since the type of pyrolysis greatly influences the product yields and composition, such data cannot thus be compared straightforwardly. Indeed, the compounds formed during the cork pyrolysis differ from those formed during wood pyrolysis. This is highlighted in the work performed by Marques and Pereira (2014) that identified and quantified the pyrolysis-derived compounds (py-products) of Cork samples (namely, *Betula pendula*, *Quercus suber*, and *Quercus cerris*) using Py-GC-MS/FID at temperatures between 550 °C and 900 °C. Their results showed that at 550–650 °C, cork bio-oil had a composition similar to a wood bio-oil but with half the amount. In contrast, at temperatures higher than 650 °C, the oxygen content in the bio-oil was reduced, and composition changed from hydrophilic pyrolysis products to a cork-specific aliphatic-rich hydrophobic oil. The chemical differences between cork and wood explain this change in behavior and are attributed to the presence of suberin in cork. Although the content of paraffin and olefins is much higher in the present work than in the said work, some compounds were similar to the ones detected by Marques and Pereira (2014). These differences could be anticipated because of the different types of pyrolysis treatment used.

The comparison of the data collected by Marques and Pereira (2014) and those obtained in the present study is given in Figure 10. The main compounds identified, including their retention time, peak area, and chemical formula, are listed in Table 2.

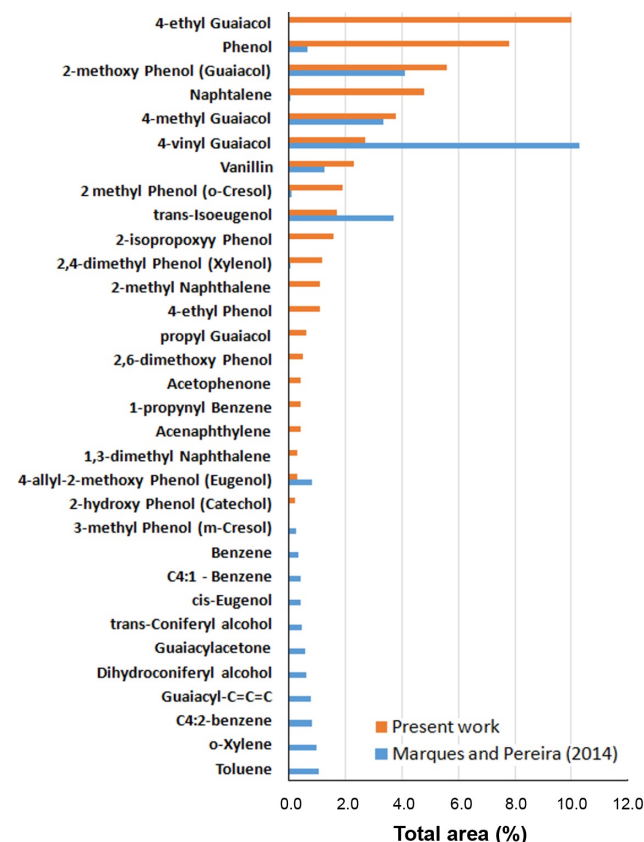


Fig. 10. Composition (aromatics and oxygenated compounds) of cork pyrolytic bio-oil obtained in the present study and the study by Marques and Pereira (2014), in terms of the percentage of total area of all detected peaks.

### 3.3.3. Solid fraction characterization

The solid fraction was characterized through elementary and proximate analysis. The results are presented in Table 3, where the HHV of the biochar is also given.



**Table 2.**

Main compounds identified by GC/MS in the condensable liquid fraction, including the total area percentage of all detected peaks, retention time, peak area, and chemical formula.

Peak	Compound	Area (%)	Retention time (s)	Peak area	Formula
1	Acetic acid	9.6	182	2.8×10 <sup>7</sup>	CH <sub>3</sub> COOH
2	Phenol	7.8	829	2.3×10 <sup>7</sup>	C <sub>6</sub> H <sub>5</sub> OH
3	Benzene, 1-propynyl-	0.4	928	1.2×10 <sup>6</sup>	C <sub>9</sub> H <sub>8</sub>
4	Acetophenone	0.4	991	1.1×10 <sup>6</sup>	C <sub>8</sub> H <sub>8</sub> O
5	Phenol, 2-methyl- (o-Cresol)	1.9	1009	5.7×10 <sup>6</sup>	C <sub>7</sub> H <sub>8</sub> O
6	Phenol, 2-methoxy- (Guaiacol)	5.6	1061	1.7×10 <sup>7</sup>	C <sub>7</sub> H <sub>8</sub> O <sub>2</sub>
7	Octanoic acid, methyl ester	1.1	1142	3.3×10 <sup>6</sup>	C <sub>9</sub> H <sub>18</sub> O <sub>2</sub>
8	Phenol, 2,3-dimethyl- (Xylenol)	1.2	1202	3.6×10 <sup>6</sup>	C <sub>8</sub> H <sub>10</sub> O
9	Naphthalene	4.8	1233	1.4×10 <sup>7</sup>	C <sub>10</sub> H <sub>8</sub>
10	Phenol, 4-ethyl-	1.1	1243	3.2×10 <sup>6</sup>	C <sub>8</sub> H <sub>10</sub> O
11	p-Methylguaiacol	3.8	1275	1.1×10 <sup>7</sup>	C <sub>8</sub> H <sub>10</sub> O <sub>2</sub>
12	2-Decanone	1.2	1277	3.5×10 <sup>6</sup>	C <sub>10</sub> H <sub>20</sub> O
13	Dodecane	1.2	1288	3.6×10 <sup>6</sup>	C <sub>12</sub> H <sub>26</sub>
14	2-Hydroxyphenol (Catechol)	0.2	1327	7.0×10 <sup>5</sup>	C <sub>6</sub> H <sub>6</sub> O <sub>2</sub>
15	Nonanoic acid, methyl ester	1.2	1335	3.5×10 <sup>6</sup>	C <sub>10</sub> H <sub>20</sub> O <sub>2</sub>
16	2-Isopropoxyphenol	1.6	1370	4.8×10 <sup>6</sup>	C <sub>9</sub> H <sub>12</sub> O <sub>2</sub>
17	p-Ethylguaiacol	10.0	1427	3.0×10 <sup>7</sup>	C <sub>9</sub> H <sub>12</sub> O <sub>2</sub>
18	1-Tridecene	0.6	1451	1.9×10 <sup>6</sup>	C <sub>13</sub> H <sub>26</sub>
19	Naphthalene, 2-methyl-	1.1	1464	3.2×10 <sup>6</sup>	C <sub>11</sub> H <sub>10</sub>
20	Tridecane	2.0	1465	5.8×10 <sup>6</sup>	C <sub>13</sub> H <sub>28</sub>
21	4-Vinylguaiacol	2.7	1488	8.0×10 <sup>6</sup>	C <sub>9</sub> H <sub>10</sub> O <sub>2</sub>
22	Decanoic acid, methyl ester	0.6	1509	1.8×10 <sup>6</sup>	C <sub>11</sub> H <sub>22</sub> O <sub>2</sub>
23	Phenol, 2,6-dimethoxy- (Syringol)	0.5	1553	1.4×10 <sup>6</sup>	C <sub>8</sub> H <sub>10</sub> O <sub>3</sub>
24	p-Propylguaiacol	0.6	1571	1.7×10 <sup>6</sup>	C <sub>10</sub> H <sub>14</sub> O <sub>2</sub>
25	1-Tetradecene	0.5	1614	1.4×10 <sup>6</sup>	C <sub>14</sub> H <sub>28</sub>
26	Tetradecane	2.6	1627	7.7×10 <sup>6</sup>	C <sub>14</sub> H <sub>30</sub>
27	Vanillin	2.3	1630	6.8×10 <sup>6</sup>	C <sub>8</sub> H <sub>8</sub> O <sub>3</sub>
28	Isoeugenol,c&t	0.3	1635	1.0×10 <sup>6</sup>	C <sub>10</sub> H <sub>12</sub> O <sub>2</sub>
29	Naphthalene, 1,3-dimethyl-	0.3	1639	9.0×10 <sup>5</sup>	C <sub>12</sub> H <sub>12</sub>
30	Undecanoic acid, methyl ester	0.5	1665	1.4×10 <sup>6</sup>	C <sub>12</sub> H <sub>22</sub> O <sub>2</sub>
31	Acenaphthylene	0.4	1680	1.3×10 <sup>6</sup>	C <sub>12</sub> H <sub>8</sub>
32	Naphthalene, 1,3-dimethyl-	0.4	1691	1.1×10 <sup>6</sup>	C <sub>12</sub> H <sub>12</sub>
33	Phenol, 2-methoxy-4-(1-propenyl)- (trans Isoeugenol)	1.7	1703	5.1×10 <sup>6</sup>	C <sub>10</sub> H <sub>12</sub> O <sub>2</sub>
34	1-Pentadecene	1.3	1765	4.0×10 <sup>6</sup>	C <sub>15</sub> H <sub>30</sub>
35	Pentadecane	3.0	1776	9.0×10 <sup>6</sup>	C <sub>15</sub> H <sub>32</sub>
36	1-Hexadecene	1.3	1906	3.8×10 <sup>6</sup>	C <sub>16</sub> H <sub>32</sub>
37	Hexadecane	3.1	1917	9.1×10 <sup>6</sup>	C <sub>16</sub> H <sub>34</sub>
38	1-Nonadecene	0.7	2041	2.0×10 <sup>6</sup>	C <sub>19</sub> H <sub>38</sub>
39	Heptadecane	2.3	2051	6.7×10 <sup>6</sup>	C <sub>17</sub> H <sub>36</sub>
40	9-Heptadecanone	0.9	2143	2.8×10 <sup>6</sup>	C <sub>17</sub> H <sub>34</sub> O
41	5-Octadecene, (E)-	1.4	2168	4.1×10 <sup>6</sup>	C <sub>18</sub> H <sub>36</sub>
42	Octadecane	3.0	2178	9.0×10 <sup>6</sup>	C <sub>18</sub> H <sub>38</sub>
43	Pentadecanoic acid, methyl ester	0.9	2206	2.7×10 <sup>6</sup>	C <sub>16</sub> H <sub>32</sub> O <sub>2</sub>
44	Cyclopentadecanone	0.7	2258	2.2×10 <sup>6</sup>	C <sub>15</sub> H <sub>28</sub> O
45	9-Octadecanone	0.6	2266	1.8×10 <sup>6</sup>	C <sub>18</sub> H <sub>36</sub> O
46	1-Nonadecene	1.5	2290	4.5×10 <sup>6</sup>	C <sub>19</sub> H <sub>38</sub>
47	Nonadecane	3.4	2299	1.0×10 <sup>7</sup>	C <sub>19</sub> H <sub>40</sub>
48	9-Hexadecenoic acid, methyl ester, (Z)-	0.8	2326	2.4×10 <sup>6</sup>	C <sub>17</sub> H <sub>32</sub> O <sub>2</sub>
49	5-Eicosene, (E)-	0.8	2407	2.3×10 <sup>6</sup>	C <sub>20</sub> H <sub>40</sub>
50	Eicosane	0.3	2415	8.8×10 <sup>5</sup>	C <sub>20</sub> H <sub>42</sub>
51	10-Heneicosene (c,t)	0.3	2522	1.0×10 <sup>6</sup>	C <sub>21</sub> H <sub>42</sub>
52	Heneicosane	1.2	2529	3.6×10 <sup>6</sup>	C <sub>21</sub> H <sub>44</sub>
53	Docosane	0.1	2617	3.0×10 <sup>5</sup>	C <sub>22</sub> H <sub>46</sub>

**Table 3.**  
Pyrolysis solid product characteristics.

Item	Value (wt%)
Carbon	90.5±2.1
Oxygen*	7.2±2.4
Hydrogen	0.9±0.1
Nitrogen	1.0±0.2
Sulfur	< 0.3
Chloride	< 0.1
	MJ kg <sup>-1</sup>
HHV	32.0±0.2

\* Calculated by difference from 100%

Elemental analysis showed that biochar obtained was a carbon-rich fuel, having a carbon content of 90% (on a dry basis). This biochar belongs to class

1 (C > 60%), based on the International Biochar Initiative (IBI) classification system, exhibiting the characteristics of high-quality biochar. The high carbon content could be explained by the high pyrolysis temperature used; increasing the pyrolysis temperature increased C content considerably but decreased H, N, and O contents in the biochar compared to those in the feedstock (Irfan et al., 2016). This could be attributed to the fact that the devolatilization removes most of the H from the biomass as the pyrolysis conversion reaction occurs. The sulfur and chloride yields were below 0.3 wt%, which could be ascribed to the low content of these elements in the cork used in the pyrolysis tests.

The fact that the gross calorific value of cork biochar was 32 MJ kg<sup>-1</sup> not only makes it an attractive fuel option but also reveals that the biochar was converted into pure carbon (graphitic structure), possessing an HHV of 32.8 MJ kg<sup>-1</sup> (Blázquez et al., 2019). The high carbon content obtained could also confirm this hypothesis (Ronse et al., 2013). The result obtained in the present study shows that, under the conditions used, the cork biochar can therefore be used as a solid fuel (Oliveira et al., 2017) due to its high calorific value. However, besides its use as solid biofuels, cork biochar may also be considered for other high-value applications, which could boost the economic viability of the slow pyrolysis process of cork residues, such as soil amelioration (Houben et al., 2013), a precursor for activated carbon production (Tan et al., 2017), combustion feedstock (Pereira and Pinho, 2013), heterogeneous catalysts for biodiesel production (Bhatia et al., 2020), and precursor for bio-oils (Pan et al., 2013). Some of these applications still require further upgrading steps to increase the economic value of this biochar (Aroso et al., 2017).

#### 4. Conclusions and Prospects

Slow pyrolysis of cork resulted in carbon char (≈60%) as well as gaseous and liquid by-products that can be promising compounds for the production of aliphatic-rich pyrolytic biofuels or as a source of olefins. The pyrolysis process was temperature-dependent and closely related to the cork composition. The major non-condensable gases included H<sub>2</sub>, CO<sub>2</sub>, CH<sub>4</sub>, and the constituents of condensable gases were alkanes and alkenes compounds in the C<sub>11</sub>-C<sub>24</sub> range. Therefore, it can be inferred that the thermal decomposition of cork in N<sub>2</sub>, in the temperature range of 400–700 °C, was governed by its chemical composition (polysaccharides, lignin, and suberin). On the other hand, cork is an excellent natural material to produce a carbonaceous solid that preserves its porous tridimensional ordered structure. This feature makes cork a promising candidate for producing ceria ecoceramics based on the pyrolyzed cork templates with a high potential for green hydrogen generation using concentrated solar energy. In addition, pyrolyzed cork ought to be regarded as a precursor for producing activated carbons suitable for both the abatement of harmful volatile organic compounds (VOCs) and the production of biopolymer materials. The pyrolysis by-products, namely the gases products, could be valorized to produce energy for the pyrolysis process, decreasing its energy needs. On the other hand, the bio-oil obtained was mainly composed of hydrocarbons that, after an upgrading process, could be used in the production of aliphatic-rich pyrolytic biofuels or as a source of olefins. The cork biochar obtained could also be used as solid fuel given its high HHV, which was very close to that of pure carbon.

Further work needs to be carried out to better understand the kinetic of cork pyrolysis and to identify the degradation mechanism of the main cork compounds. This could contribute to improving the yield and quality of the products and the efficiency of the overall process. Moreover, efforts should be put into increasing the conversion efficiency of the process and scrutinizing its economic aspects.

#### Acknowledgements

The authors are thankful to Amorim Cork Composites S.A. for providing the cork samples. A.M. and P.O.S. acknowledge the research fellowships offered by FCT (Fundação para a Ciência e a Tecnologia, Portugal) in the frame of the H2CORK project (grant numbers PTDC/CTM-ENE/6762/2014, POCI-01-0145-FEDER-016862). The authors also thank Rita Sousa and Amélia Caldeira for performing the biochar analysis at the Laboratory of Bioenergy and Biorefineries of LNEG. This work was developed within the scope of the project INIESC – National Research



Infrastructure in Solar Energy Concentration National Infrastructure (grant number ALT20-03-0145-FEDER-022113). The authors would also like to acknowledge the EU through the seventh framework program for the financial support of this work under the STAGE-STE project (grant number 609837) and the SFERA II project (grant number 312643).

## References

- [1] Al-Kassir, A., Gañán-Gómez, J., Mohamad, A.A., Cuerda-Correa, E.M., 2010. A study of energy production from cork residues: sawdust, sandpaper dust, and triturated wood. *Energy*. 35(1), 382-386.
- [2] APCOR's Cork Yearbook 2020.
- [3] APCOR's Information Bureau: Cork Sector in Numbers 2019.
- [4] Aroso, M.I., Araújo, A.R., Pires, R.A., Reis, R.L., 2017. Cork: current technological developments and future perspectives for this natural, renewable, and sustainable material. *ACS Sustainable Chem. Eng.* 5(12), 11130-11146.
- [5] Basu, P., 2018. Chapter 5-Pyrolysis, in biomass gasification, pyrolysis and torrefaction-practical design and theory, 3<sup>rd</sup> Ed. Academic Press, London, UK. pp. 155-187.
- [6] Bento, M.F., Cunha, M.A., Moutinho, A.M.C., Pereira, H., Fortes, M.A., 1992. A mass spectrometry study of thermal dissociation of cork. *Int. J. Mass Spectrom. Ion Processes*. 112(2-3), 191-204.
- [7] Bhatia, S.K., Gurav, R., Choi, T.R., Kim, H.J., Yang, S.Y., Song, H.S., Park, J.Y., Park, Y.L., Han, Y.H., Choi, Y.K., Kim, S.H., Yoon, J.J., Yang, Y.H., 2020. Conversion of waste cooking oil into biodiesel using heterogeneous catalyst derived from cork biochar. *Bioresour. Technol.* 302, 122872.
- [8] Blázquez, G., Pérez, A., Iáñez-Rodríguez, I., Martínez-García, C., Calero, M., 2019. Study of the kinetic parameters of thermal and oxidative degradation of various residual materials. *Biomass Bioenergy*. 124, 13-24.
- [9] Cardoso, B., Mestre, A.S., Carvalho, A.P., Pires, J., 2008. Activated carbon derived from cork powder waste by KOH activation: preparation, characterization, and VOCs adsorption. *Ind. Eng. Chem. Res.* 47(16), 5841-5846.
- [10] Carriço, C., Ribeiro, H.M., Marto, J., 2018. Converting cork by-products to ecofriendly cork bioactive ingredients: novel pharmaceutical and cosmetics applications. *Ind. Crops. Prod.* 125, 72-84.
- [11] Castola, V., Marongiu, B., Bighelli, A., Floris, C., Lai, A., Casanova, J., 2005. Extractives of cork (*Quercus suber* L.): chemical composition of dichloromethane and supercritical CO<sub>2</sub> extracts. *Ind. Crops Prod.* 21(1), 65-69.
- [12] Chen, H., 2015. Lignocellulose biorefinery engineering: principles and applications, Woodhead Publishing Series in Energy: Number 74. Woodhead Publishing Ltd., Cambridge, UK.
- [13] Costa, R., Lourenço, A., Oliveira, V., Pereira, H., 2019. Chemical characterization of cork, phloem, and wood from different *Quercus suber* provenances and trees. *Heliyon*. 5(12), e02910.
- [14] Dhyani, V., Bhaskar, T.A., 2018. A comprehensive review on the pyrolysis of lignocellulosic biomass. *Renew. Energy*. 129, 695-716.
- [15] Encinar, J.M., Gonzalez, J.F., Gonzalez, J., 2000. Fixed-bed pyrolysis of *Cynara cardunculus* L. product yields and compositions. *Fuel Proc. Technol.* 68(3), 209-222.
- [16] EPA - United States Environmental Protection Agency, Air Emission Measurement Center (EMC), EMC Promulgated test methods, 2017. Method 11 - Determination of hydrogen sulfide content of fuel gas streams in petroleum refineries.
- [17] FAO - State of the World's Forests Report, 2020. The food and agriculture organization (FAO) of the United Nations, Rome, Italy.
- [18] Fernandes, E.M., Correló, V.M., Chagas, J.A.M., Mano, J.F., Reis, R.L., 2011. Properties of new cork-polymer composites: advantages and drawbacks as compared with commercially available fibreboard materials. *Compos. Struct.* 93(12), 3120-3129.
- [19] Fernandes, E.M., Correló, V.M., Mano, J.F., Reis, R.L., 2015. Cork-polymer biocomposites: mechanical, structural and thermal properties. *Mater. Design*. 82, 282-289.
- [20] Ferreira, R., Garcia, H., Sousa, A.F., Petkovic, M., Lamosa, P., Freire, C.S., Silvestre, A.J., Rebelo, L.P.N., Pereira, C.S., 2012. Suberin isolation process from cork using ionic liquids: characterisation of ensuing products. *New J. Chem.* 36(10), 2014-2024.
- [21] Fukuyama, T., Maetani, S., Ryu I., 2014. 3.22 Carbonylation and Decarbonylation Reactions, in *Comprehensive Organic Synthesis: Second Edition*. Elsevier Ltd. 3, 1073-1100.
- [22] Gil, L., 1997. Powder cork waste: an overview. *Biomass Bioenergy*. 13, 59-61.
- [23] Gil, L., 2009. Cork composites: a review. *Materials*. 2(3), 776-789.
- [24] Guedes, R.E., Luna, A.S., Rodrigues Torres, A.R., 2018. Operating parameters for bio-oil production in biomass pyrolysis: a review. *J. Anal. Appl. Pyrolysis*. 129, 134-149.
- [25] Haq, I., Qaisar, K., Nawaz, A., Akram, F., Mukhtar, H., Zohu, X., Xu, Y., Mumtaz, M.W., Rashid, U., Ghani, W.A.W.A.K., Choong, T.S.Y., 2021. Advances in valorization of lignocellulosic biomass towards energy generation. *Catalysts*. 11(3), 309.
- [26] Houben, D., Evrard, L., Sonnet, P., 2013. Beneficial effects of biochar application to contaminated soils on the bioavailability of Cd, Pb, and Zn and the biomass production of rapeseed (*Brassica napus* L.). *Biomass Bioenergy*. 57, 196-204.
- [27] Hu, X., Gholizadeh, M., 2019. Biomass pyrolysis: a review of the process development and challenges from initial researches up to the commercialization stage. *J. Energy Chem.* 39, 109-143.
- [28] Iliopoulou, E.F., Triantafyllidis, K.S., Lappas, A.A., 2019. Overview of catalytic upgrading of biomass pyrolysis vapors toward the production of fuels and high-value chemicals. *Rev.: Energy Environ.* 8(1), e322.
- [29] Irfan, M., Chen, Q., Yue, Y., Pang, R., Lin, Q., Zhao, X., Chen, H., 2016. Co-production of biochar, bio-oil, and syngas from halophyte grass (*Achnatherum splendens* L.) under three different pyrolysis temperatures. *Bioresour. Technol.* 211, 457-463.
- [30] Kan, T., Strezov, V., Evans, T.J., 2016. Lignocellulosic biomass pyrolysis: a review of product properties and effects of pyrolysis parameters. *Renew. Sust. Energy Rev.* 57, 1126-1140.
- [31] Lagorce-Tachon, A., Mairesse, F., Karbowiak, T., Gougeon, R.D., Bellat, J.P., Sliwa, T., Simon, J.M., 2018. Contribution of image processing for analyzing the cellular structure of cork. *J. Chemom.* 32(1), e2988.
- [32] Le Barbenchon, L., Girardot, J., Kopp, J.B., Viot, P., 2018. Strain rate effect on the compressive behaviour of reinforced cork agglomerates. *EPJ Web Conf.* 183, 03018.
- [33] Leite, C., Pereira, H., 2017. Cork-containing barks-a review. *Front. Mater.* 3, 63.
- [34] Lu, Q., Yang, X.L., Zhu, X.F., 2008. Analysis on chemical and physical properties of bio-oil pyrolyzed from rice husk. *J. Anal. Appl. Pyrolysis*. 82(2), 191-198.
- [35] Marques, A.V., Pereira, H., 2014. Aliphatic bio-oils from corks: a Py-GC/MS study. *J. Anal. Appl. Pyrolysis*. 109, 29-40.
- [36] Martins, C.I., Gil, V., 2020. Processing-structure-properties of cork polymer composites. *Front. Mater.* 7, 297.
- [37] Mateus, M.M., Bordado, J.C., Santos, R.G., 2016. Potential biofuel from liquefied cork-Higher heating value comparison. *Fuel*. 174, 114-117.
- [38] Mohan, D., Pittman Jr, C.U., Steele, P.H., 2006. Pyrolysis of wood/biomass for bio-oil: a critical review. *Energy Fuels*. 20(3), 848-889.
- [39] Nunes, L.J.R., Matias, J.C.O., Catalão, J.P.S., 2013. Energy recovery from cork industrial waste: production and characterisation of cork pellets. *Fuel*. 113, 24-30.
- [40] Oliveira, F.A.C., Barreiros, M.A., Haeussler, A., Caetano, A.P., Mouquinhó, A.I., Oliveira e Silva, P.M.O., Novais, R.M., Pullar, R.C., Abanades, S., 2020. High-performance cork-templated ceria for solar thermochemical hydrogen production via two-step water-splitting cycles. *Sustain. Energy Fuels*. 4(6), 3077-3089.
- [41] Oliveira, F.R., Patel, A.K., Jaisi, D.P., Adhikari, S., Lu, H., Khanal, S.K., 2017. Environmental application of biochar: current status and perspectives. *Bioresour. Technol.* 246, 110-122.
- [42] Órfão, J.J., Antunes, F.J., Figueiredo, J.L., 1999. Pyrolysis kinetics of lignocellulosic materials-three independent reactions model. *Fuel*. 78(3), 349-358.

- [43] Pan, S., Pu, Y., Foston, M., Ragauskas, A.J., 2013. Compositional characterization and pyrolysis of Loblolly pine and Douglas-fir bark. *Bioenergy Res.* 6(1), 24-34.
- [44] Pereira, C.C., Pinho, C., 2013. Determination of fluidized bed combustion kinetic and diffusive data of four wood chars from the central region of Portugal. *Energy Fuels.* 27(12), 7521-7530.
- [45] Pereira, H., 1988. Chemical composition and variability of cork from *Quercus suber* L. *Wood Sci. Technol.* 22(3), 211-218.
- [46] Pereira, H., 1992. The thermochemical degradation of cork. *Wood Sci. Technol.* 26(4), 259-269.
- [47] Pereira, H., 2013. Variability of the chemical composition of cork. *BioResources.* 8(2), 2246-2256.
- [48] Pereira, H., 2015. The rationale behind cork properties: a review of structure and chemistry. *BioResour.* 10(3), 6207-6229.
- [49] Pinto, F., Paradela, F., Carvalheiro, F., Duarte, L.C., Costa, P., André, R., 2018. Co-pyrolysis of pre-treated biomass and wastes to produce added value liquid compounds. *Chem. Eng. Trans.* 65, 211-216.
- [50] Ronsse, F., Nachenius, R.W., Prins, W., 2015. Carbonization of biomass, in Pandey, A., Bhaskar, T., Stocker, M., Sukumaran, R. (Eds.) *Recent Advances in Thermochemical Conversion of Biomass*, 1<sup>st</sup> Ed.; Elsevier, Amsterdam, pp. 293-324.
- [51] Ronsse, F., van Heck, S., Dickinson, D., Prins, W., 2013. Production and characterization of slow pyrolysis biochar: Influence of feedstock type and pyrolysis conditions. *GCB Bioenergy.* 5(2), 104-115.
- [52] Rosa, M.E., Fortes, M.A., 1988. Thermogravimetric analysis of cork. *J. Mater. Sci. Lett.* 7, 1064-1065.
- [53] Şen, A., Marques A.V., Gominho J., Pereira, H., 2012. Study of thermochemical treatments of cork in the 150-400 °C range using colour analysis and FTIR spectroscopy. *Ind. Crops Prod.* 38, 132-138.
- [54] Şen, A., Van den Bulcke, J., Defoirdt, N., Van Acker, J., Pereira, H., 2014. Thermal behaviour of cork and cork components. *Thermochim. Acta.* 582, 94-100.
- [55] Silva, S.P., Sabino, M.A., Fernandes, E.M., Correlo, V.M., Boesel, L.F., Reis, R.L., 2005. Cork: properties, capabilities and applications. *Int. Mater. Rev.* 50(6), 345-365.
- [56] Sousa, A.F., Pinto, P.C., Silvestre, A.J., Neto, C.P., 2006. Triterpenic and other lipophilic components from industrial cork byproducts. *J. Agric. Food Chem.* 54(18), 6888-6893.
- [57] Tan, X.F., Liu, S.B., Liu, Y.G., Gu, Y.L., Zeng, G.M., Hu, X., Wang, X.J., Liu, S.H., Jiang, L.H., 2017. Biochar as potential sustainable precursors for activated carbon production: multiple applications in environmental protection and energy storage. *Bioresour. Technol.* 227, 359-372.
- [58] Teixeira, J., Almeida, A., Freitas, M., Pilão, R., Neto, P., Pereira, I., Ribeiro, A., Ribeiro, A., 2017. Pyrolysis of cork granules: influence of operating variables on char yield. *Int. J. Chem. Eng.* 9, 16-22.
- [59] Uçar, S., Karagöz, S., 2009. The slow pyrolysis of pomegranate seeds: the effect of temperature on the product yields and bio-oil properties. *J. Anal. Appl. Pyrolysis.* 84(2), 151-156.
- [60] Wang, C., Du, Z., Pan, J., Li, J., Yang, Z., 2007. Direct conversion of biomass to bio-petroleum at low temperature. *J. Anal. Appl. Pyrolysis.* 78(2), 438-444.
- [61] Wang, G., Dai, Y., Yang, H., Xiong, Q., Wang, K., Zhou, J., Li, Y., Wang, S., 2020. A review of recent advances in biomass pyrolysis. *Energy Fuels.* 34(12), 15557-15578.
- [62] Wen, J.L., Xue, B.L., Sun, S.L., Sun, R.C., 2013. Quantitative structural characterization and thermal properties of birch lignins after auto-catalyzed organosolv pre-treatment and enzymatic hydrolysis. *J. Chem. Technol. Biotechnol.* 88(9), 1663-1671.
- [63] Xia, C., Cai, L., Zhang, H., Zuo, L., Shi, S., Lam, S., 2021. A review on the modeling and validation of biomass pyrolysis with a focus on product yield and composition. *Biofuel Res. J.* 8(1), 1296-1315.
- [64] Yang, H., Yan, R., Chin, T., Liang, D.T., Chen, H., Zheng, C., 2004. Thermogravimetric analysis-fourier transform infrared analysis of palm oil waste pyrolysis. *Energy Fuel.* 18(6), 1814-1821.
- [65] Yao, F., Wu, Q., Lei, Y., Guo, W., Xu, Y., 2008. Thermal decomposition kinetics of natural fibers: activation energy with dynamic thermogravimetric analysis. *Polym. Degrad. Stab.* 93(1), 90-98.
- [66] Yona, A.M.C., Budija, F., Kričej, B., Kutnar, A., Pavlič, M., Pori, P., Tavzes, C., Petrič, M., 2014. Production of biomaterials from cork: liquefaction in polyhydric alcohols at moderate temperatures. *Ind. Crops Prod.* 54, 296-301.
- [67] Zanzi, R., 2001. *Pyrolysis of biomass*. PhD. dissertation, Royal Institute of Technology, Stockholm, Sweden.
- [68] Zhang, S., Yang, X., Zhang, H., Chu, C., Zheng, K., Ju, M., Liu, L., 2019. Liquefaction of biomass and upgrading of bio-oil: a review. *Molecules.* 24(12), 2250.



**Dr. Paula Costa** obtained her Ph.D. in Chemical Engineering at the Faculty of Science and Technology of the New University of Lisbon, in 2006, in the field of production of liquid and gaseous hydrocarbons by plastic waste pyrolysis. She is a researcher at the National Laboratory for Energy and Geology and an invited professor at the Faculty of Sciences of the University of Lisbon teaching Hydrogen and New Energy Vectors. Her research activities are mainly in the area of thermochemical conversion of wastes and alternative fuels production using pyrolysis, gasification, liquefaction, and hydrogenation processes.



**Fernando de Almeida Costa Oliveira (F.A.C. Oliveira)** is a principal researcher with "habilitation" in the Unit of Materials for Energy at the National Laboratory of Energy and Geology (LNEG). He was awarded a Ph.D. degree in Materials Science (1992) from the Technical University of Delft (The Netherlands). Since 2020, he has been the coordinator of the scientific research area on the development of materials for the renewable energies of LNEG and invited professor of Materials Science and Engineering in the Department of Mechanical Engineering of Instituto Superior de Engenharia de Lisboa (ISEL) of the Polytechnic Institute of Lisbon (IPL). He has co-authored over 160 papers and holds two patents. He is currently working on developing materials for solar concentrated power systems.



**Dr. M. Alexandra Barreiros** obtained her Ph.D. in the field of Applied Physics from the New University of Lisbon in 2003. She is a researcher working at the National Laboratory of Energy and Geology in the Unit of Materials for Energy. Her domains of specialization and scientific interests are X-ray spectrometry and diffraction techniques, scanning electron microscopy and X-ray microanalysis, ion beam analysis, including nuclear microprobe techniques. At present, the main research activity is the development of analytical methodologies to characterize functional materials for solar cells. Another field of Dr. Barreiros' current research is the characterization of CeO<sub>2</sub>-based catalysts used for H<sub>2</sub>O and CO<sub>2</sub> splitting to produce chemical fuels *via* direct solar thermochemical fuel production.



**Dr. Ana Mouquinho** completed her Ph.D. in Sustainable Chemistry at the Faculty of Science and Technology of the New University of Lisbon in 2019. During her Ph.D., she conducted a multidisciplinary project covering areas such as Organic Synthesis and Materials Science. From July 2018 to October 2019, Ana was a research fellow at the National Laboratory of Energy and Geology (LNEG). Since March 2020, she has been a postdoctoral fellow at CENIMAT/i3N centre, working on photonic-enhanced flexible perovskite solar cells (PSCs). In parallel, she is also an invited adjunct professor at the state-run college of higher education dedicated to nautical studies - Escola Superior Náutica Infante D. Henrique - lecturing the subjects of Chemical-Physics, Industrial Chemistry, and Analytical Chemistry.



**Pedro Oliveira e Silva** earned his master's degree in Energy and Environmental Engineering at the Faculty of Sciences of the University of Lisbon (FCUL) in 2017. During his master's dissertation, he developed his work at the National Laboratory of Energy and Geology (LNEG) in biofuel production. From June 2018 to April 2019, Pedro was a research fellow at LNEG, working on solar thermochemical production of hydrogen based on cork ecoceramics. From July 2019 to March 2021, he worked as an Environmental

Technician in a Portuguese non-governmental organization. Nowadays, he is engaged in the area of safety and health at work after having completed a course on Occupational Safety Superior Technician.



**Dr. Filipe Paradela** is an auxiliary researcher in the National Laboratory of Energy and Geology (LNEG) in Lisbon, Portugal. Dr. Paradela received a Ph.D. in Chemical Engineering from the Faculty of Science and Technology of the New University of Lisbon in 2013. He has published 20 research articles in academic journals with an h-index of 7 with over 380 citations. His current research interests are biofuel production and upgrading *via* pyrolysis, HTL, and HDO from several sources. His Google Scholar profile can be found at the following link: <https://scholar.google.com/citations?user=gifrzkwAAAAJ&hl=en>.